



The Stem Cell Factor Sox2 Is a Positive Timer of Oligodendrocyte Development in the Postnatal Murine Spinal Cord

Sheng Zhang^{1,2} · Abeer Rasai¹ · Yan Wang^{1,2} · Jie Xu¹ · Peter Bannerman^{1,3} · Daffcar Erol¹ · Danayit Tsegaye¹ · Aijun Wang^{1,4} · Athena Soulika^{1,5} · Xiangjiang Zhan⁶ · Fuzheng Guo^{1,2,7} 

Received: 26 December 2017 / Accepted: 23 March 2018 / Published online: 5 April 2018
© Springer Science+Business Media, LLC, part of Springer Nature 2018

Abstract

Myelination in the central nervous system takes place predominantly during the postnatal development of humans and rodents by myelinating oligodendrocytes (OLs), which are differentiated from oligodendrocyte progenitor cells (OPCs). We recently reported that Sox2 is essential for developmental myelination in the murine brain and spinal cord. It is still controversial regarding the role of Sox2 in oligodendroglial lineage progression in the postnatal murine spinal cord. Analyses of a series of cell- and stage-specific Sox2 mutants reveal that Sox2 plays a biphasic role in regulating oligodendroglial lineage progression in the postnatal murine spinal cord. Sox2 controls the number of OPCs for subsequent differentiation through regulating their proliferation. In addition, Sox2 regulates the timing of OL differentiation and modulates the rate of oligodendrogenesis. Our experimental data prove that Sox2 is an intrinsic positive timer of oligodendroglial lineage progression and suggest that interventions affecting oligodendroglial Sox2 expression may be therapeutic for overcoming OPC differentiation arrest in dysmyelinating and demyelinating disorders.

Keywords Sox2 · Myelination · Oligodendrocyte differentiation · Oligodendrocyte progenitor cells (OPCs) · Proliferation · Neural stem cells

Introduction

Oligodendrocytes are CNS myelin-forming cells. Oligodendroglial lineage progression encompasses multiple

sequential steps including OPC generation, migration, proliferation, differentiation into premyelinating OLs (i.e., OL differentiation), and myelination by myelinating OLs [1]. Perturbation of any steps could result in myelination impairment.

In the CNS, the SRY (sex-determining region Y)-box 2, Sox2 is highly expressed in NSCs [2, 3] and maintains the properties of neural stem cells (NSCs) and progenitor cells [4, 5]. In line with its role in NSC/progenitor cells, recent data have shown that overexpression of Sox2 converts differentiated astrocytes and OPCs back into neural progenitor cells in vivo under certain circumstances [6–8]. However, there are “conflicting” observations in the current literatures regarding the role of Sox2 in the spinal cord oligodendrocyte development. Hoffmann and colleagues reported that Sox2 is dispensable for OPC proliferation and migration, but essential for OL differentiation and myelination in the perinatal spinal cord [9]. A recent study by Zhao et al. reported that Sox2 seems dispensable for OL differentiation and myelination in the postnatal spinal cord [10]. However, this study employed animal models of non-cell-specific Sox2 deletion driven by the actin promoter. More recently, we used animal models of cell-specific Sox2 deletion driven by the Sox10 promoter (Sox10-Cre:Sox2^{fl/fl}) and found that Sox2 is required for

✉ Fuzheng Guo
fzguo@ucdavis.edu

¹ Institute for Pediatric Regenerative Medicine, Shriners Hospitals for Children/UC Davis School of Medicine, Sacramento, CA 95817, USA

² Department of Neurology, School of Medicine, UC Davis, Davis, CA 95817, USA

³ Department of Cell Biology and Human Anatomy, School of Medicine, UC Davis, Davis, CA 95817, USA

⁴ Department of Surgery, School of Medicine, UC Davis, Davis, CA 95817, USA

⁵ Department of Dermatology, School of Medicine, UC Davis, Davis, CA 95817, USA

⁶ Key Laboratory of Animal Ecology and Conservation Biology, Institute of Zoology, Chinese Academy of Sciences, Beijing 100101, China

⁷ Department of Neurology, UC Davis School of Medicine, c/o Shriners Hospitals for Children, Room 601A, 2425 Stockton Blvd, Sacramento, CA 95817, USA

developmental myelination in the murine spinal cord and brain [11]. These discrepant observations prompted us to revisit the role of Sox2 in oligodendroglial lineage progression in the postnatal spinal cord by leveraging our cell- and stage-specific animal models of Sox2 deletion.

To this end, we used *Sox10-Cre:Sox2^{fl/fl}* animal model to constitutively delete Sox2 in OPCs and tamoxifen-inducible *Pdgfra-CreER^{T2}:Sox2^{fl/fl}* to delete Sox2 in OPCs at the neonatal ages. In addition, we used *Cnp-Cre:Sox2^{fl/fl}* animal model to constitutively delete Sox2 in differentiation-committed OPCs and their progenies and tamoxifen-inducible *Plp-CreER^{T2}:Sox2^{fl/fl}* to time-conditionally delete Sox2 in differentiation-committed OPCs and their progenies. Through analysis and comparison of oligodendrocyte lineage phenotypes among these Sox2 mutants, we concluded that Sox2 is an intrinsic bi-phasic regulator of oligodendroglial proliferation and differentiation during developmental myelination of postnatal murine spinal cord, as we recently reported in the postnatal brain [11].

Results

Our recent data show that Sox2 is expressed in OPCs and upregulated in newly differentiated OLs during CNS developmental myelination [11]. Here, we employed the genetic approach of *Cre-loxP*-mediated labeling and demonstrated that Sox2 was expressed in all OPCs regardless of their CNS regional origins (Fig. 1).

Sox2 Is Specifically and Efficiently Deleted in OPCs in the Spinal Cord of *Sox10-Cre:Sox2^{fl/fl}* Mutants

Sox10 expression is absent from embryonic NSCs (i.e., neuroepithelial cells) and starts in OPCs immediately after OPC specification from NSCs at ~embryonic 12.5 days (E12.5) in the mouse spinal cord [12]. Accordingly, *Sox10-Cre*-mediated Sox2 deletion was observed in all PDGFR α ⁺ OPCs (Fig. 2a1–a2) but not in the neuroepithelial cells at the ventricular zone (boxed areas in Fig. 2a1–a2).

OPC Proliferation and Migration in the Embryonic Spinal Cord of *Sox10-Cre:Sox2^{fl/fl}* Mutants

Interestingly, Sox2-deficient embryonic OPCs migrated and proliferated normally in the spinal cord of *Sox10-Cre:Sox2^{fl/fl}* embryos, indistinguishable from Sox2-intact OPCs in Sox2^{fl/fl} controls (arrowheads in Fig. 2c1 vs Fig. 2c2, Fig. 2d) at E15.5, ~

3 days after OPC specification. Our results suggest that Sox2 is dispensable for OPC proliferation and migration in the embryonic spinal cord, which is consistent with the previous data [9].

Hypomyelination in the Adult Spinal Cord of *Sox10-Cre:Sox2^{fl/fl}* Mutants

Our recent data show that *Sox10-Cre:Sox2^{fl/fl}* mutants display tremors and ataxia (indicators of hypomyelination) and impaired performance on accelerating Rotarod [11] at P28, an approximate time point that oligodendrocyte differentiation and developmental myelination are close to completion in the murine spinal cord. In this study, we found that myelination impairment persisted into the adult ages, as assessed by diminished density of myelinated axons in CST of *Sox10-Cre:Sox2^{fl/fl}* mutants at P60, compared with littermate control mice (Fig. 3). Our previous and current data suggest that Sox2 is essential for developmental myelination in the murine spinal cord.

Time Course Analysis of OPC Proliferation and OL Differentiation in the Postnatal Spinal Cord of *Sox10-Cre:Sox2^{fl/fl}* Mutants

Hypomyelination in *Sox10-Cre:Sox2^{fl/fl}* mutant spinal cord indicates defects in the oligodendroglial lineage progression. To quantify cell number at the different developmental stages of oligodendroglial lineage cells, we used Sox10 or Olig2 to label all oligodendroglial lineage cells (OPCs and OLs), Sox10 (or Olig2) and PDGFR α to label OPCs, Sox10 (or Olig2) and CC1 to label differentiated OLs, and APC/TCF712 to label newly differentiated premyelinating OLs. We first confirmed that Sox2 was completely and specifically deleted from oligodendroglial lineage cells in the postnatal spinal white matter, as evidenced by the absence of Sox2 in Olig2⁺ oligodendroglial lineage cells (arrowheads in Fig. 4a left vs right panels) in the spinal cord of *Sox10-Cre:Sox2^{fl/fl}* mutants.

At P3, the number of Sox10⁺ oligodendroglial lineage cells (Fig. 4b), Sox10⁺CC1⁺ OLs (Fig. 4c), and Sox10⁺PDGFR α ⁺ OPCs (Fig. 4e) was significantly decreased in *Sox10-Cre:Sox2^{fl/fl}* mutants compared with that in non-Cre controls. We used Sox10 and Ki67 to identify cycling OPCs (Fig. 4g, arrowheads) and found that the number of proliferating OPCs was also significantly reduced in the mutant white matter (Fig. 4f). We have shown that TCF712 [13] and APC [14] are upregulated and co-expressed in newly formed premyelinating OLs and dramatically downregulated in mature myelinating OLs. Therefore, the number of TCF712⁺APC⁺ cells at any given time provides a quantitative indication of the rate of OL generation from OPCs, or

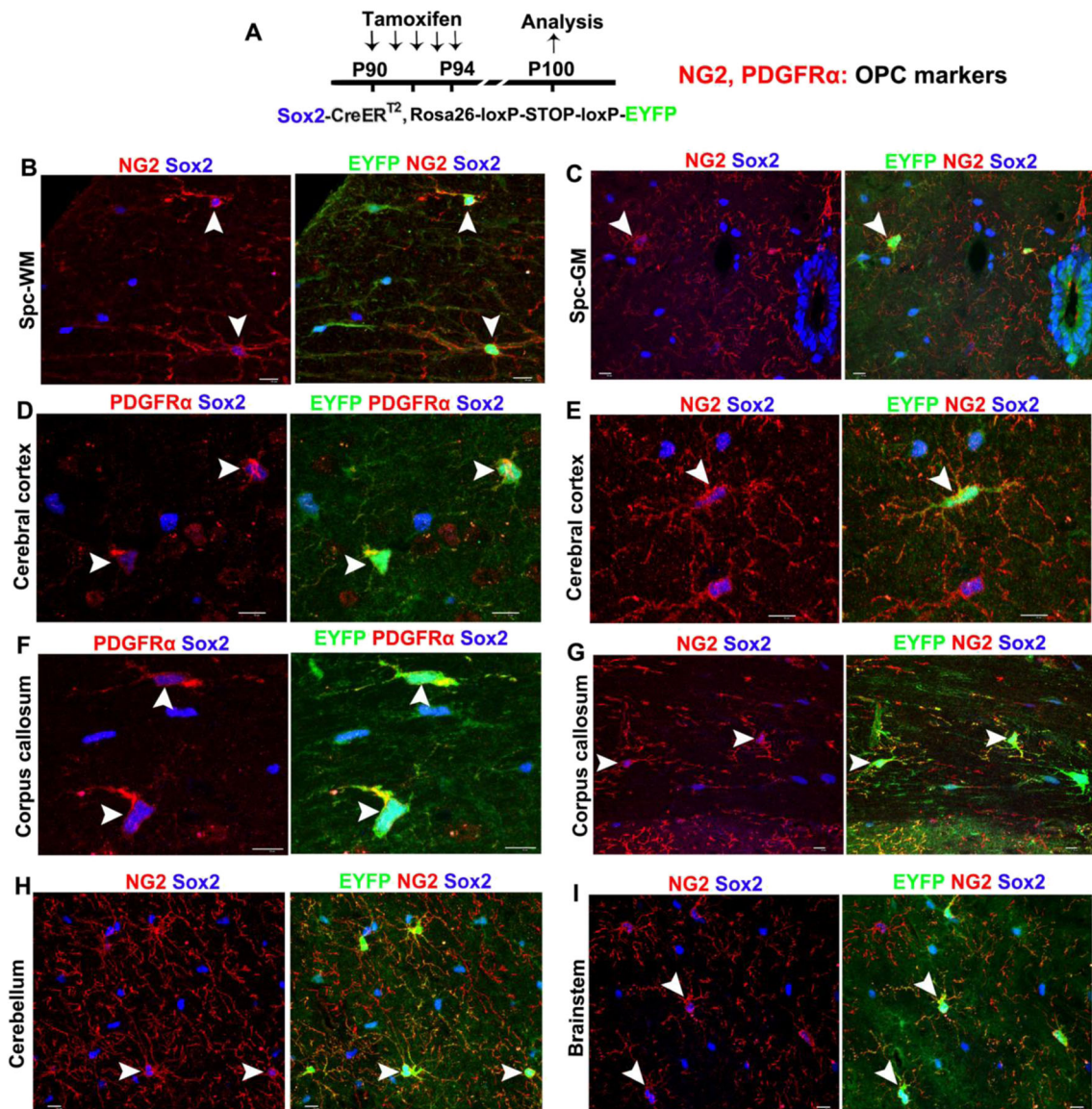


Fig. 1 Sox2 is ubiquitously expressed in all adult OPCs throughout the CNS regions. **a** Transgenic mice and experimental designs. Double transgenic mice carrying *Sox2-CreER^{T2}* and *Rosa26-loxP-STOP-loxP-EYFP* were injected intraperitoneally with tamoxifen daily from P90 through P94, and CNS tissues were processed at P100 for immunohistochemical analysis of EYFP and the OPC markers NG2 and PDGFR α . Note that the *Sox2-CreER^{T2}* transgene is homologously knocked in the locus of endogenous *Sox2* gene. Therefore, tamoxifen inducible EYFP expression is a bona fide indicator of endogenous Sox2 promoter activity. **b–i** Triple immunohistochemistry of reporter EYFP,

endogenous Sox2, and OPC markers PDGFR α (or NG2) unequivocally demonstrate that Sox2 is expressed in adult OPCs in the spinal cord white matter (WM) (**b**) and gray matter (GM) (**c**), cerebral cortex (**d**, **e**), corpus callosum (**f**, **g**), cerebellum (**h**), and brainstem (**i**). Arrowheads point to the examples of PDGFR α (or NG2)⁺ OPCs that have both endogenous Sox2 (blue) and transgenic EYFP expression. Note that 100% of EYFP⁺ cells (including astrocytes and OPCs) are Sox2 positive, validating that EYFP is a reliable indicator of endogenous Sox2 expression. Over 90% of NG2⁺ (or PDGFR α)⁺ OPCs are EYFP⁺ using the tamoxifen injection paradigm (see the “Materials and methods” section). Scale bars = 10 μ m

oligodendrogenesis. Our quantification data showed a 75% reduction of TCF712⁺APC⁺ newly formed premyelinating OLs in the white matter of *Sox10-Cre:Sox2^{fl/fl}* mutants compared with non-Cre controls (Fig. 4h–i). These data indicate that Sox2 positively regulates oligodendroglial lineage progression and the rate of oligodendrogenesis in the early postnatal spinal cord.

A recent study reported that oligodendroglial lineage progression was normal by the second postnatal week

(P14) in the spinal cord of Sox2 ubiquitously ablated mice (*Cag-CreERTM:Sox2^{fl/fl}*) [10]. However, our recent data demonstrated that oligodendroglial lineage progression was persistently impaired in the spinal cord of *Sox10-Cre:Sox2^{fl/fl}* mice even at later states of spinal cord development [11]. In line with our recent histological data of diminished number of OPCs and OLs, RT-qPCR quantification showed that the mRNA levels of OL lineage genes, *Sox10*, *Pdgfra*, *Plp-E3b*, *Cnp*, *CC1*, and *Enpp6*, and

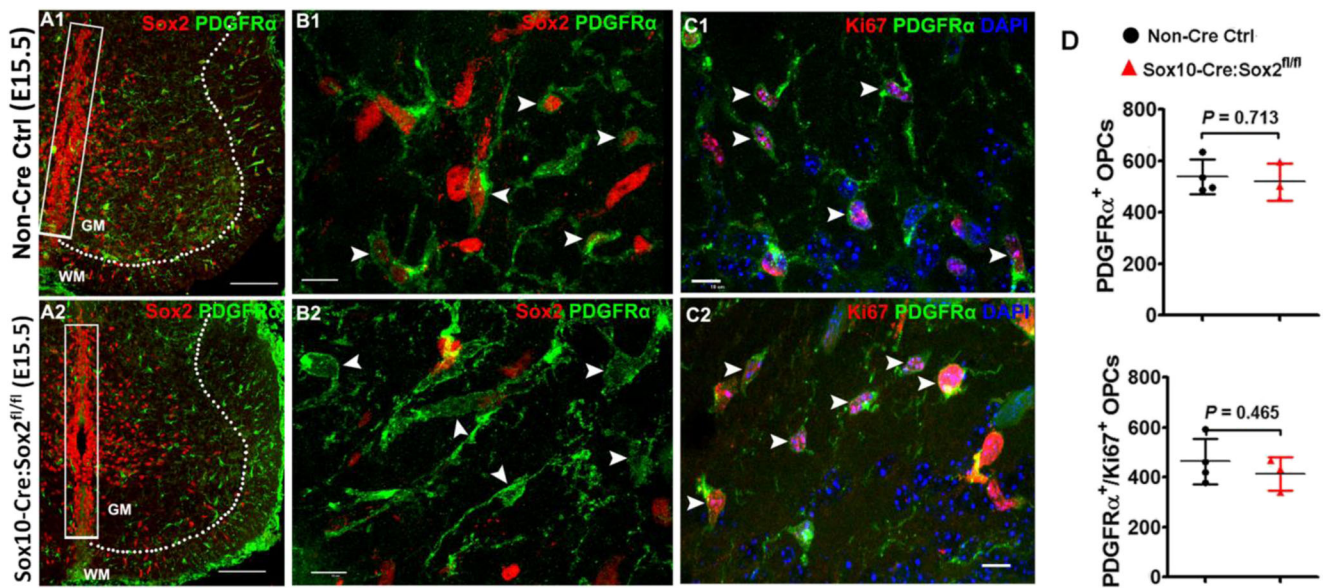


Fig. 2 Sox2 ablation does not affect OPC migration and proliferation during embryonic spinal cord development. **a1–a2** Low-magnification confocal images showing that Sox2-deficient PDGFR α^+ embryonic OPCs are generated and migrate normally into the primitive gray and white matter (**a2**) in a similar manner to those in Sox2-intact OPCs (**a1**). Dashed lines demarcate gray matter (GM) and white matter (WM). Note that Sox2 is preserved in the neuroepithelial cells (boxed areas) aligning the ventricular zones in E15.5 Sox10-Cre, Sox2^{fl/fl} (Sox2 cKO) spinal cord. **b1–b2** High-magnification confocal images showing

similar distribution and equivalent density of PDGFR α^+ embryonic OPCs in the white matter of E15.5 spinal cord of Sox2 cKO (**b2**, arrowheads) and non-Cre control (**b1**, arrowheads). **c1–c2** The distribution and density of Ki67⁺PDGFR α^+ -proliferating OPCs are similar in Sox2 cKO (**c2**, arrowheads) spinal cord to those in non-Cre controls (**c1**, arrowheads) at E15.5. Blue in **c1–c2** is DAPI nuclear staining. **d** Densities of OPCs and proliferating OPCs in the primitive WM of spinal cord at E15.5. Two tailed Student's *t* test, $t_{(5)} = 0.3897$ PDGFR α^+ , $t_{(5)} = 0.7903$ PDGFR α^+ Ki67 $^+$. Scale bar: **a1–a2**, 100 μ m; **b1–c2**, 10 μ m

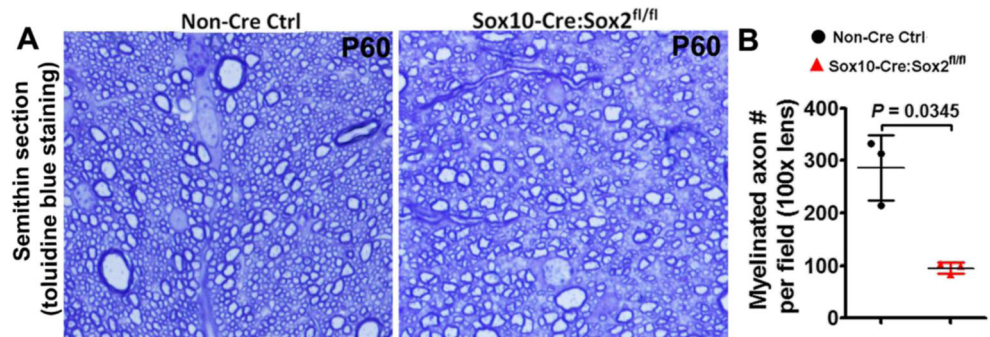
OPC-specific gene were significantly decreased in the P19 spinal cord of Sox10-Cre:Sox2^{fl/fl} mice compared with non-Cre controls (Fig. 5a). Western blot verified the reduced protein level of myelin genes MBP and CNP (Fig. 5b). Therefore, our previous and current data suggest that oligodendroglial lineage progression is persistently impaired even during the later stages of spinal cord development.

Collectively, the time-course data obtained from Sox10-Cre:Sox2^{fl/fl} mutants indicate that Sox2 is indispensable for oligodendroglial lineage progression during developmental myelination in the murine spinal cord.

Time Course Analysis of OPC Proliferation and OL Differentiation in Postnatal Spinal Cord of Tamoxifen Inducible *Pdgfra-CreER^{T2}:Sox2^{fl/fl}* Mutants

One can argue that the diminished OPC and OL population in the postnatal Sox10-Cre:Sox2^{fl/fl} mutants is the secondary effects of Sox2 deletion in embryonic OPCs on postnatal development. To exclude this possibility, we employed a time-conditional paradigm to elicit Sox2 deletion. In this regard, we generated *Pdgfra-CreER^{T2}:Sox2^{fl/fl}* (Sox2 cKO) transgenic hybrids. Tamoxifen was administered at P1, P2, and P3, and

Fig. 3 Sox2 disruption impairs axonal myelination in the adult spinal cord of Sox10-Cre:Sox2^{fl/fl} mutants. **a** Representative images of toluidine blue staining of myelin in the corticospinal tract (CST) at P60. Scale bar = 10 μ m. **b** Quantification of myelinated axon numbers per field. Two-tailed Student's *t* test with Welch's correction, $t_{(2)} = 5.231$



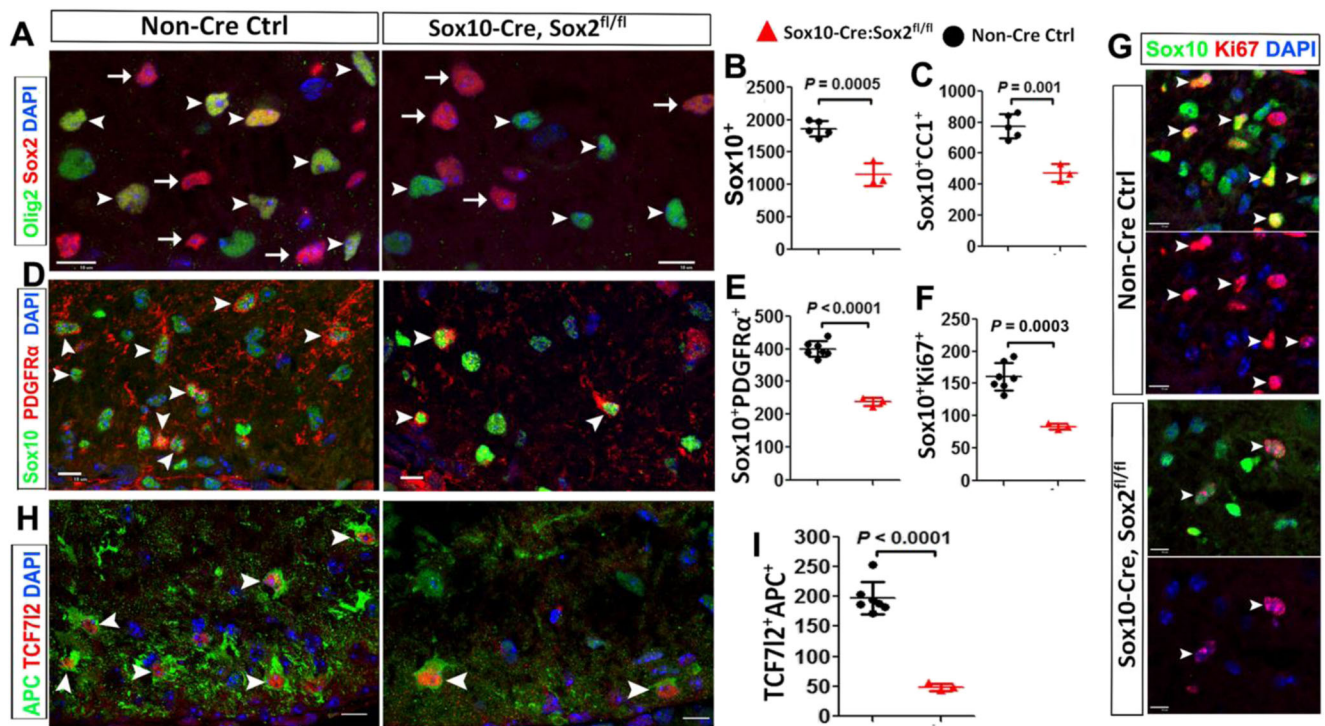


Fig. 4 Sox2 deletion diminishes OPC number and proliferation and reduces the density of differentiated OLs in the spinal cord at postnatal day 3 (P3). **a** Representative confocal images showing that Sox2 is expressed in Olig2⁺ oligodendroglial lineage cells (OPCs and OLs) in non-Cre controls and absent from Olig2⁺ cells in *Sox10-Cre, Sox2^{fl/fl}* (Sox2 cKO) mice at P3 (**a**, arrowheads). Note that Sox2⁺/Olig2⁺ astrocytic lineage cells (arrows) are equivalently present in both control and Sox2 cKO white matter. **b–c** Density (# per mm²) of Sox10⁺ oligodendroglial lineage cells and Sox10⁺CC1⁺ differentiated OLs in the spinal white matter at P3 (two-tailed Student’s *t* test, $t_{(6)} = 6.763$ Sox10⁺, $t_{(6)} = 5.73$ Sox10⁺CC1⁺). **d–e** Representative confocal images of the pan-

oligodendroglial lineage marker Sox10 and the OPC marker PDGFR α and quantification. Two-tailed Student’s *t* test, $t_{(8)} = 10.93$ Sox10⁺PDGFR α ⁺. Arrowheads point to examples of Sox10⁺PDGFR α ⁺ OPCs. **f–g** Density (per mm²) and representative images of Sox10 and Ki67. Two-tailed Student’s *t* test, $t_{(8)} = 6.02$. Arrowheads point to examples of Sox10⁺Ki67⁺ cells. **h–i** Representative confocal images depicting TCF712⁺APC⁺ newly differentiated premyelinating OLs (**h**, arrowheads) and the density (per mm²) of TCF712⁺APC⁺ cells (**i**). Two-tailed Student’s *t* test, $t_{(8)} = 9.246$. Blue, DAPI⁺ nuclei. Scale bars: 10 μ m, applied to all

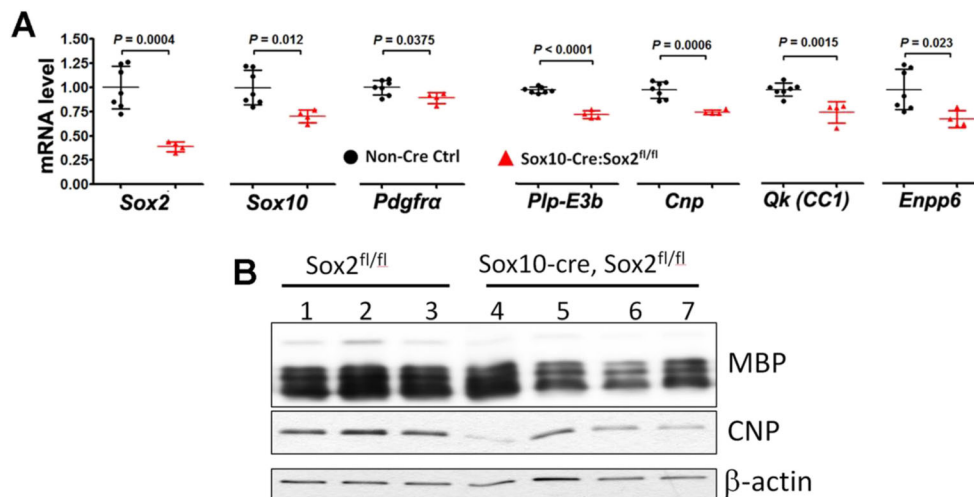


Fig. 5 Reduced expression of myelin-related genes in the spinal cord *Sox10-Cre:Sox2^{fl/fl}* mutants at P19. **a** RT-qPCR quantification of spinal cord mRNA levels of *Sox2*, *Sox10*, *Pdgfra*, *Plp-E3b* (exon3b-containing proteolipid protein), *Cnp*, *Qk* (also known as CC1), and premyelinating OL-specific *Enpp6* at P19. Gene expression was normalized to the internal control *Hsp90*, and the level in non-Cre Ctrl was set to 1. *N* = 7 non-

Cre control (black circles) and 4 Sox2 cKO (red triangles), two-tailed Student’s *t* test [$t_{(9)} = 5.397$ *Sox2*, $t_{(9)} = 3.131$ *Sox10*, $t_{(9)} = 2.437$ *Pdgfra*, $t_{(9)} = 11.71$ *Plp-E3b*, $t_{(9)} = 5.145$ *Cnp*, $t_{(9)} = 4.487$ *Qk*, and $t_{(9)} = 2.734$ *Enpp6*]. **b** Western blotting of myelin proteins MBP and CNP, and the loading control β -actin in the P19 spinal cord

spinal cord was harvested at P8 and P26 (Fig. 6a). About 91.5% and 49.6% PDGFR α^+ OPCs were Sox2-positive at P8 and P26, respectively in the *Pdgfra-CreER^{T2}:Sox2* cKO mice (Fig. 6b, c) whereas nearly 100% of PDGFR α^+ OPCs were positive for Sox2 at both time points in the non-Cre controls (Fig. 6c). Olig2⁺PDGFR α^+ OPC population (Fig. 6d, arrowheads) was significantly reduced in the spinal cord of *Pdgfra-CreER^{T2}:Sox2^{fl/fl}* mutants at both P8 and P26, compared with that of non-Cre littermate controls (41% reduction at P8 and 17% at P26) (Fig. 6e), suggesting that Sox2 is required for maintaining OPC population during postnatal spinal cord development.

The decreased OPC population would lead to reduced number of differentiated oligodendrocytes. Accordingly, we found that OL differentiation and myelination were impaired in the spinal cord of *Pdgfra-CreER^{T2}:Sox2* cKO mice, as evidenced by decreased number of Olig2⁺CC1⁺ OLs (Fig. 6d arrows and Fig. 6f) and hypomyelination (Fig. 6g). Consistently, the mRNA levels of myelin genes *Mbp*, *Plp-E3b*, and *Mog* (Fig. 6h) and the density of *Plp* mRNA⁺ oligodendrocytes (Fig. 6i, j) were significantly reduced in *Pdgfra-CreER^{T2}:Sox2* cKO mice at P8. Furthermore, the number of APC⁺TCF712⁺ newly formed premyelinating OLs was significantly reduced in the spinal cord of *Pdgfra-CreER^{T2}:Sox2* cKO mice compared with non-Cre littermate controls at both P8 and P26 (Fig. 6k, right). Collectively, these data indicate that Sox2 promotes OPC population supply for subsequent OL differentiation.

OPC population is maintained by proliferation, apoptosis, or both. We then analyzed OPC proliferation and apoptosis. Our data showed that the percentage of Ki67⁺ cycling OPCs was significantly reduced at both P8 (by 42%) and P26 (by 43%) in the spinal cord of *Pdgfra-CreER^{T2}:Sox2* cKO mice (Fig. 7b, c, d), which is confirmed by 2 h EdU pulse labeling (Fig. 7e). However, we found no alterations in the density of active Caspase 3⁺ apoptotic cells in the spinal cord of *Pdgfra-CreER^{T2}:Sox2* cKO mice in comparison to non-Cre controls at P8 and P26 (Fig. 7f). Of note, our in vivo data are different from those collected from in vitro system in which Sox2 ablation significantly increases caspase-dependent OPC apoptosis [10].

Taken together, the data obtained from the time-conditional *Pdgfra-CreER^{T2}:Sox2^{fl/fl}* mutants unequivocally demonstrate that Sox2 plays a crucial role in OPC proliferation and that Sox2 ablation in postnatal OPCs reduces their proliferative capacity, leading to a diminished density of OPCs and OLs.

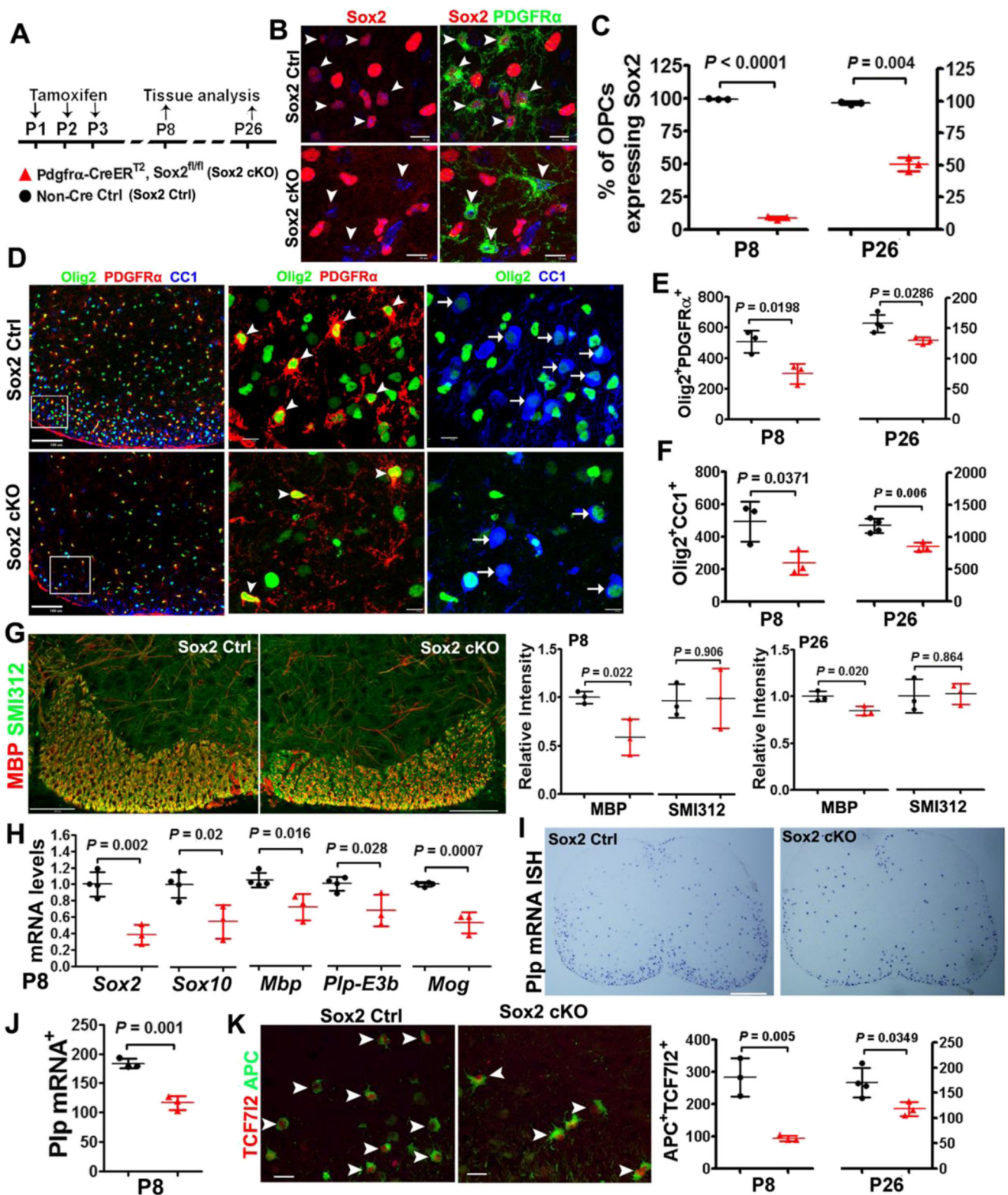
Delayed OL Differentiation in the Spinal Cord of *Cnp-Cre:Sox2^{fl/fl}* Mutants—a Time-Course Analysis

To determine the role of Sox2 in OL differentiation without compromising OPC population, we analyzed the spinal cord

Fig. 6 Sox2 regulates OPC population supply and impacts OL differentiation in the murine postnatal spinal cord. **a** Transgenic mice and experimental designs. *Pdgfra-CreER^{T2}, Sox2^{fl/fl}* (Sox2 cKO) neonates and non-Cre controls were injected subcutaneously with tamoxifen at P1, P2, and P3 once a day, and spinal cords were analyzed on P8 and P26. **b** Representative confocal images showing Sox2 is expressed in PDGFR α^+ OPCs in non-Cre Ctrl (upper panels, arrowheads) and absent from PDGFR α^+ OPCs in Sox2 cKO (lower panels, arrowheads) spinal cord at P8. Scale bars = 10 μ m. **c** Percentage of PDGFR α^+ OPCs that express Sox2 in the spinal white matter at P8 and P26. Two-tailed Student's *t* test [$t_{(4)} = 116.2$ P8, $t_{(4)} = 15.25$ P26]. **d** Triple immunohistochemistry of pan-oligodendroglial lineage marker Olig2, OPC marker PDGFR α , and OL marker CC1 in Sox2 Ctrl and cKO spinal cord at P8. Boxed areas in the first column are shown at higher magnification at the right. Arrowheads and arrows point to examples of Olig2⁺PDGFR α^+ OPCs and Olig2⁺CC1⁺ OLs, respectively. Scale bars, 100 μ m in the first column images, 10 μ m in the rest images. **e** Quantification (per mm²) of Olig2⁺PDGFR α^+ OPCs in spinal cord WM. Two-tailed Student's *t* test [$t_{(4)} = 3.758$ P8, $t_{(5)} = 3.044$ P26]. **f** Density (per mm²) of Olig2⁺CC1⁺ OLs in the spinal cord WM. Two-tailed Student's *t* test [$t_{(4)} = 3.077$ P8, $t_{(5)} = 4.568$ P26]. **g** Representative confocal images of MBP and axonal marker SMI312 (scale bars = 100 μ m) in the ventral medial white matter of spinal cord (left) and quantification of MBP and SMI312 relative intensity (right) at P8 and P26. Two-tailed Student's *t* test, $t_{(4)} = 3.644$ MBP and $t_{(4)} = 0.126$ SMI312 at P8; $t_{(4)} = 3.699$ MBP and $t_{(4)} = 0.183$ SMI312 at P26. **h–i** Representative bright-field images of *Plp* mRNA in situ hybridization (ISH) of spinal cord and quantification at P8. Two-tailed Student's *t* test, $t_{(4)} = 7.941$. Scale bars = 200 μ m. **j** RT-qPCR quantification of spinal cord mRNA levels of indicated genes at P8. The mRNA level was normalized to the internal control *Hsp90*, and the level in Sox2 Ctrl was set to 1. Two-tailed Student's *t* test [$t_{(5)} = 5.880$ *Sox2*, $t_{(5)} = 3.346$ *Sox10*, $t_{(5)} = 3.552$ *Mbp*, $t_{(5)} = 3.072$ *Plp-E3b*, $t_{(5)} = 7.408$ *Mog*]. **k** Representative confocal images of APC and TCF712 in the P8 spinal cord (left) and quantification (right). Scale bars = 20 μ m. Two-tailed Student's *t* test, $t_{(4)} = 5.526$ P8, $t_{(5)} = 2.833$ P26

of *Cnp-Cre:Sox2^{fl/fl}* mice in which Cre-recombinase mediates gene deletion primarily in post-mitotic differentiation-committed OPCs and later stages of OLs [15–21].

At P8, immunohistochemistry confirmed that Sox2 was specifically deleted in Olig2⁺ oligodendroglial lineage cells in the spinal cord of *Cnp-Cre:Sox2^{fl/fl}* mutants (Fig. 8b, c). The density of Olig2⁺ pan-oligodendroglial lineage cells (Fig. 8d) and Olig2⁺CC1⁺ differentiated OLs (Fig. 8e) was significantly decreased in the spinal white matter (WM) of *Cnp-Cre:Sox2^{fl/fl}* mutants compared with non-Cre control and one-allele deletion (*Cnp-Cre:Sox2^{fl/+}*). In sharp contrast to the reduced OPC population in *Sox10-Cre:Sox2^{fl/fl}* mutants, the number of Olig2⁺PDGFR α^+ OPCs was indistinguishable between the three groups (Fig. 8f), indicating that Sox2 is primarily ablated in post-mitotic OPCs and later stages of OLs. Consistent with the histological data, we observed significant decreases in the mRNA levels of the pan-oligodendroglial lineage marker *Sox10*, mature OL-enriched genes *Plp-E3b* (*exon3b-containing Plp*), *Mbp*, *Mag*, and *Mog* (Fig. 8g), and premyelinating OL-enriched genes *Enpp6*, *Tcf712*, *Bcas1*, *Ugt8a*, and *Bmp4* (Fig. 8h), indicating that OL differentiation is inhibited in the P8 spinal cord of *Cnp-Cre:Sox2^{fl/fl}* mice.



Our recent data report that oligodendrocyte number and myelin gene expression are normal in the P14 spinal cord of *Cnp-Cre:Sox2^{fl/fl}* mice [11]. In the current study, we showed that OPC density was unchanged in the P14 spinal cord of *Cnp-Cre:Sox2^{fl/fl}* mice compared with that in the

non-Cre controls (Fig. 8i). Interestingly, the number of APC⁺/TCF712⁺ newly formed premyelinating OLs (Fig. 8k, arrowheads) was significantly decreased in the spinal cord WM and GM of *Cnp-Cre:Sox2^{fl/fl}* mice at P14 (Fig. 8j), indicating that the rate of oligodendrogenesis is

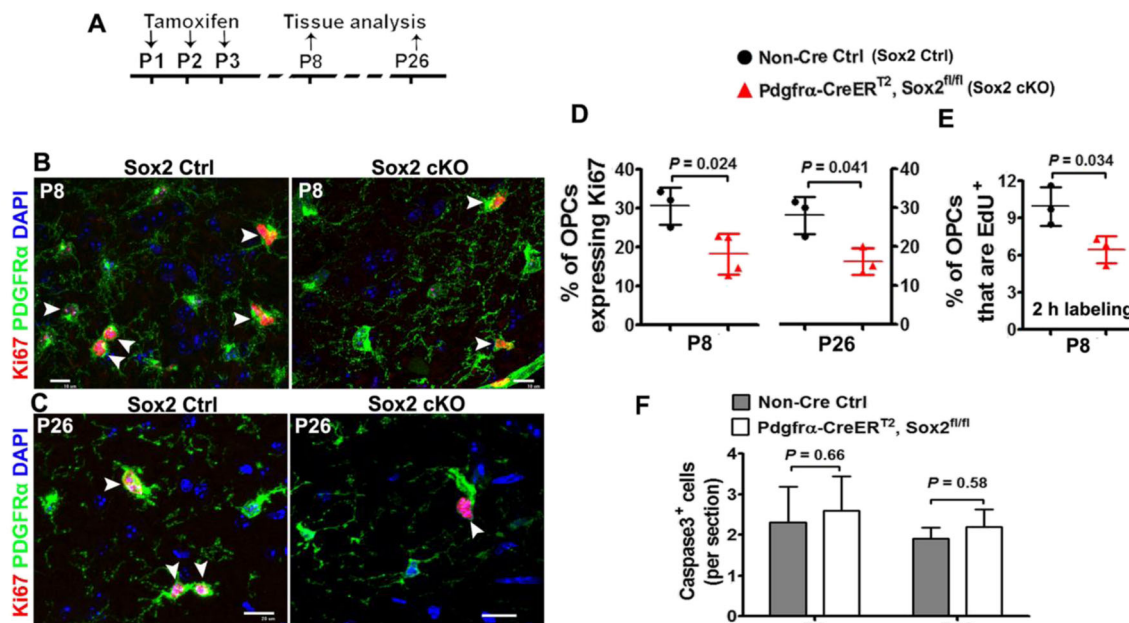


Fig. 7 Sox2 regulates OPC proliferation in the postnatal mouse spinal cord. **a** Transgenic mice and experimental designs for panels **b–e**. Thymidine analog EdU was injected intraperitoneally into Sox2 Ctrl and cKO mice 2 h before tissue harvesting. **b–c** Representative confocal images showing reduction of Ki67⁺PDGFR α ⁺ cycling OPCs in the white matter of spinal cord at P8 (**b**) and P26 (**c**). Arrowheads point to Ki67⁺PDGFR α ⁺ proliferating cells. Scale bars = 10 μ m. **d**

impaired. Consistently, myelination was inhibited in the spinal cord at P8 (Fig. 9a, b) and seemed normal in the adult of *Cnp-Cre:Sox2^{fl/fl}* mice (Fig. 9c, d). Accelerating Rotarod test showed that *Cnp-Cre:Sox2^{fl/fl}* mutants still exhibited impaired motor coordination at the adult age compared with non-Cre control mice (Fig. 9e), which is presumably due to the myelin abnormalities in the peripheral nervous system.

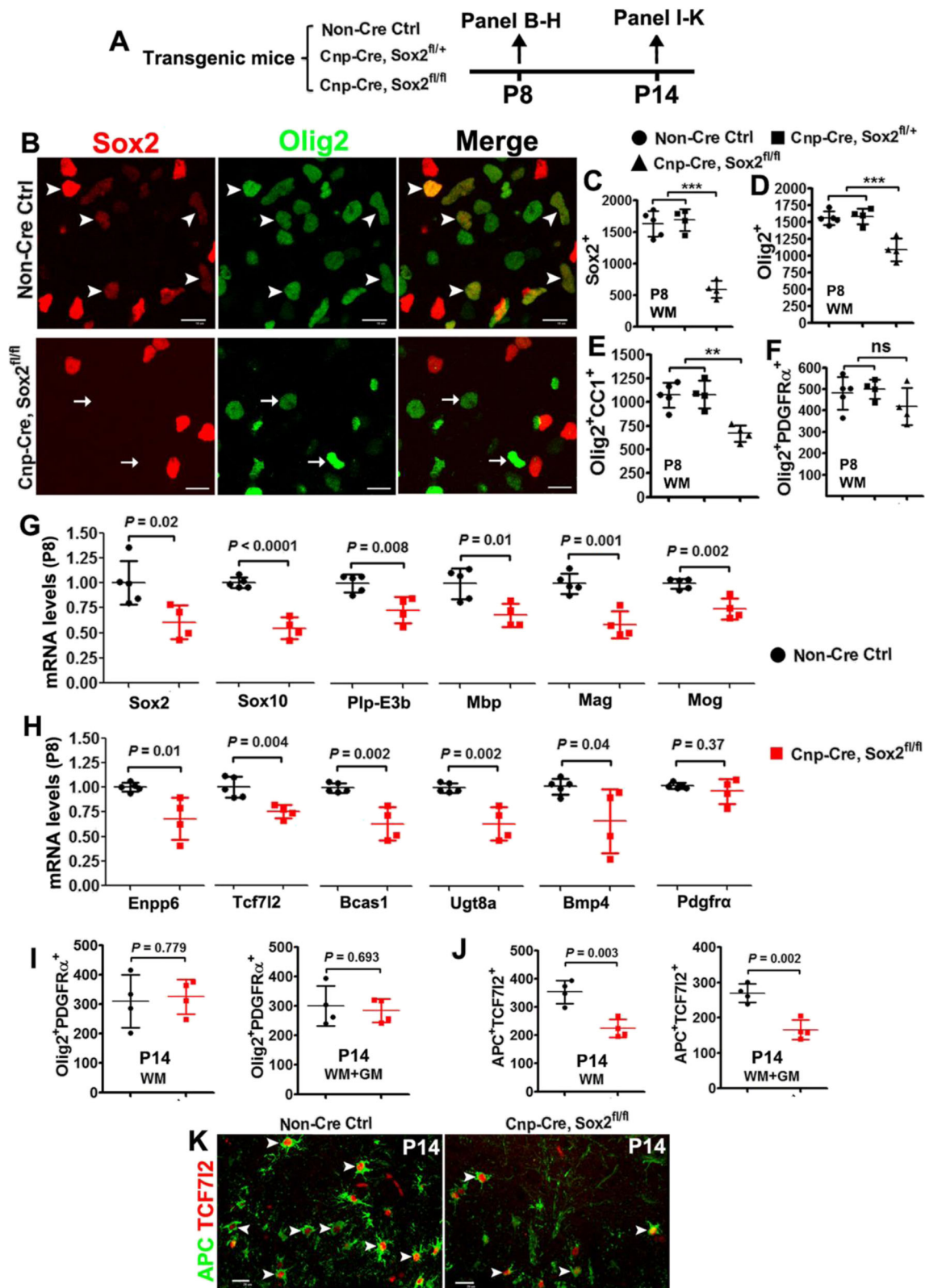
Taken together, time-course analyses of *Cnp-Cre:Sox2^{fl/fl}* transgenic hybrids suggest that Sox2 additionally regulates the timing of oligodendrocyte differentiation and enhances the rate of oligodendrocyte generation.

Reduced Rate of Oligodendrocyte Generation in the P14 Spinal Cord of *Plp-CreER^{T2}:Sox2^{fl/fl}* Mutants

To corroborate the conclusion that Sox2 enhances the rate of oligodendrocyte generation, we created the tamoxifen-inducible, time-conditional *Plp-CreER^{T2}:Sox2^{fl/fl}* transgenic mice. Tamoxifen was injected to *Plp-CreER^{T2}:Sox2^{fl/fl}* mice and non-Cre littermate controls at P10, P11, and P13, and spinal tissues were assessed at P14 (Fig. 10a). Sox2 and Olig2 immunostaining confirmed that Sox2 was deleted in most Olig2⁺ oligodendroglial

lineage cells (Fig. 10b). Our quantification data showed that Olig2⁺/PDGFR α ⁺ OPCs were similar (Fig. 10c) whereas Olig2⁺/CC1⁺ OLs were reduced in the spinal cord

Fig. 8 Sox2 positively regulates the timing of OL differentiation in the postnatal mouse spinal cord. **a** Transgenic mice and experimental designs. **b** Representative confocal images of Sox2 and pan-oligodendroglial marker Olig2 in the white matter of P8 spinal cord. Scale bars = 10 μ m. Note that Sox2 is expressed in Olig2⁺ cells in non-Cre Ctrl (upper panels, arrowheads) and absent from most Olig2⁺ cells in *Cnp-Cre:Sox2^{fl/fl}* mice (arrows in the lower panels). **c–f** Quantification of marker-positive cells in the white matter of P8 spinal cord of non-Cre Ctrl, *Cnp-Cre:Sox2^{fl/fl}* (one-allele KO) and *Cnp-Cre:Sox2^{fl/fl}* (Sox2 cKO) mice. One-way ANOVA, $F_{(2,10)} = 52.18$ $P < 0.0001$ Sox2⁺, $F_{(2,10)} = 19.16$ $P = 0.0004$ Olig2⁺, $F_{(2,10)} = 1.429$ $P = 0.285$ Olig2⁺PDGFR α ⁺, $F_{(2,10)} = 14.80$ $P = 0.001$ Olig2⁺CC1⁺. Tukey's post-hoc test was used for pairwise comparisons, ** $P < 0.001$, *** $P < 0.0001$, ns, not significant. **g–h** RT-qPCR quantification of mRNA expression of indicated genes in P8 spinal cord. mRNA level was normalized to the internal control *Hsp90*, and the level in Sox2 Ctrl was set to 1. Two-tailed Student's *t* test [$t_{(7)} = 2.957$ *Sox2*, $t_{(7)} = 8.307$ *Sox10*, $t_{(7)} = 3.660$ *Plp-E3b*, $t_{(7)} = 3.386$ *Mbp*, $t_{(7)} = 5.252$ *Mag*, $t_{(7)} = 4.782$ *Mog*, $t_{(7)} = 3.331$ *Enpp6*, $t_{(7)} = 4.129$ *Tcf7l2*, $t_{(7)} = 4.688$ *Beas1*, $t_{(7)} = 3.950$ *Ugt8a*, $t_{(7)} = 2.383$ *Bmp4*, $t_{(7)} = 0.950$ *Pdgfr α*]. **i** Densities (per mm²) of Olig2⁺PDGFR α ⁺ OPCs in the WM and whole spinal cord (WM + GM) at P14. Two-tailed Student's *t* test [$t_{(6)} = 0.293$ WM, $t_{(6)} = 0.415$ WM + GM]. **j–k** Quantification and representative confocal images showing substantial reduction of APC⁺TCF7l2⁺ premyelinating OLs in *Cnp-Cre:Sox2^{fl/fl}* spinal cord at P14. Scale bars = 10 μ m. Two-tailed Student's *t* test [$t_{(6)} = 4.935$ WM, $t_{(6)} = 5.448$ WM + GM]. Arrowheads point to APC⁺TCF7l2⁺ premyelinating OLs



of *Plp-CreER^{T2}:Sox2^{fl/fl}* mice although this reduction did not reach statistical significance (Fig. 10d). In line with the data derived from P14 *Cnp-Cre:Sox2^{fl/fl}* hybrids, the number of APC⁺TCF712⁺ newly formed premyelinating

OLs (Fig. 10e, arrowheads) was significantly reduced in the spinal cord (WM and GM) of *Plp-CreER^{T2}:Sox2^{fl/fl}* mice (Fig. 10f), indicating that Sox2 ablation perturbs the rate of oligodendrocyte generation.

Discussion

The current study resolved a key question regarding the role of Sox2 in the oligodendroglial lineage progression in the postnatal murine spinal cord. Two previous studies reported discrepant observations. Using the *Sox10-Cre:Sox2^{fl/fl}* model to constitutively delete Sox2 in OPCs, Hoffmann and colleagues demonstrated that Sox2 is required for spinal cord myelination [9]. Axonal myelination occurs predominantly during postnatal development in the CNS of both human and rodents. Unfortunately, this study did not analyze spinal myelination beyond the neonatal ages. A subsequent study reported that Sox2 seems dispensable for myelination in the postnatal spinal cord [10]. However, this study used a non-cell-specific Sox2 deletion paradigm. In the current study, we analyzed myelination in the postnatal spinal cord of the cell-specific Sox2 mutants (*Sox10-Cre:Sox2^{fl/fl}*) and conclude that Sox2 is indispensable for spinal cord myelination. The experimental data from the current and our previous studies [11] suggest that Sox2 is an intrinsic positive regulator for CNS myelination, weakening a CNS region-specific (brain vs spinal cord) role of Sox2 in developmental myelination.

In the CNS, Sox2 is highly expressed in NSCs and down-regulated or absent upon differentiation into neural progenitors [2]. Recent studies have reached the consensus that OPCs

express Sox2 in the embryonic and early postnatal CNS in vivo [9, 10, 22]. However, whether OPCs express Sox2 in the adult CNS is still controversial [10, 23]. By leveraging *Cre-LoxP*-based genetic labeling (*Sox2-CreER^{T2}:Rosa-loxP-STOP-loxP-EYFP*), we demonstrate that adult OPCs from different CNS regions exhibit endogenous Sox2 promoter activity and express Sox2 albeit at a lower level, thus arguing against a CNS region-dependent Sox2 expression in adult OPCs. This notion is consistent with recent single-cell RNA-seq data demonstrating that adult OPCs in different CNS regions are homogenous at the transcription level [21]. At the functional level, our previous and current data have unequivocally demonstrated that Sox2 is essential for OPC proliferation in the postnatal brain and spinal cord. It is well-established that OPCs are uniformly distributed throughout CNS regions and represent the largest population of proliferating cells in the adult CNS [24], and adult OPCs are responsible for oligodendrogenesis albeit at a slower rate, myelin turnover, and/or adaptive myelination [25–27]. It is plausible to speculate that Sox2 regulates the homeostasis of adult OPCs, adult oligodendrogenesis, and/or adaptive myelination. Future studies are needed to prove or falsify this prediction.

Our recent data [11] report that oligodendrocyte number and myelin gene expression are unchanged at P14 in the spinal cord of *Cnp-Cre:Sox2^{fl/fl}* mutants compared to non-Cre controls. Based on these observations, one can argue that Sox2 is

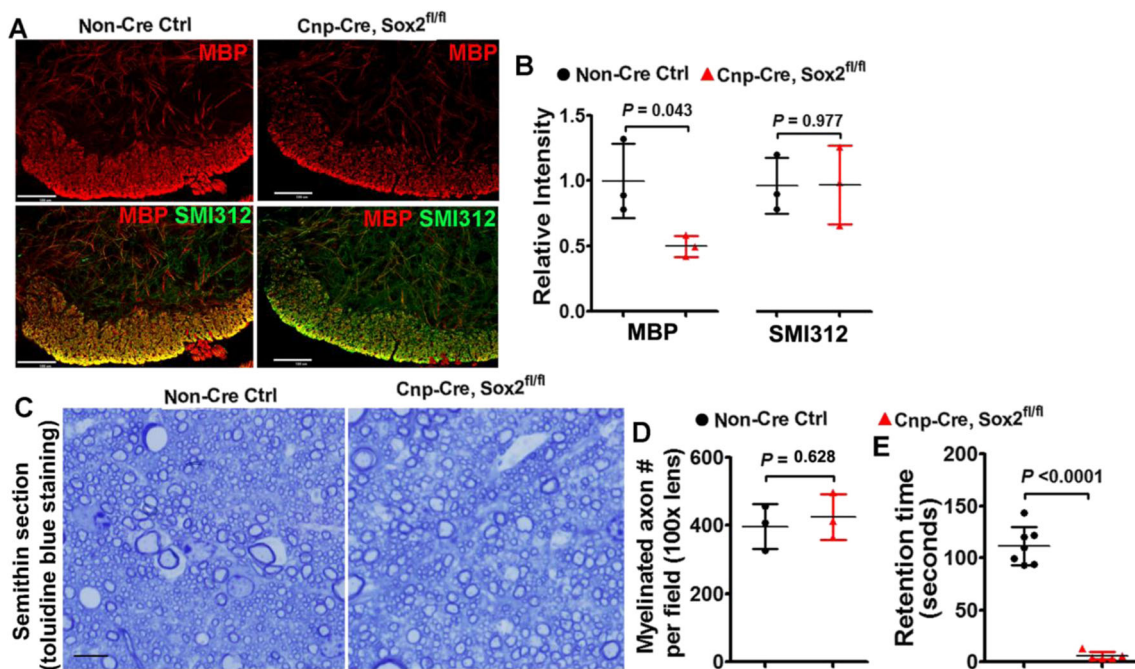


Fig. 9 Myelination assessment in the spinal cord of *Cnp-Cre:Sox2^{fl/fl}* mutants at P8 and P60. **a** Immunohistochemistry of MBP and axonal marker SMI312 in the ventral medial white matter at P8; scale bar = 100 μ m. Note that the SMI312⁺ axons are highly myelinated in the ventral medial white matter of spinal cord at P8, thus rendering the overlapped images yellow. **b** Quantification of the relative intensity of MBP and SMI312 in the ventral medial white matter at P8. Two-tailed

Student's *t* test, $t_{(4)} = 2.922$ MBP, $t_{(4)} = 0.030$ SMI312. **c–d** Representative images of toluidine blue staining of myelin on semithin (500 nm) sections in the corticospinal tract at P60 (**c**, scale bar = 10 μ m) and quantification of myelination axon numbers (**d**). Two-tailed Student's *t* test, $t_{(4)} = 0.524$. **e** Retention time on the accelerating rotarod of *Cnp-Cre:Sox2^{fl/fl}* mutant and control mice at P60. Two-tailed Student's *t* test with Welch's correction, $t_{(6)} = 14.85$

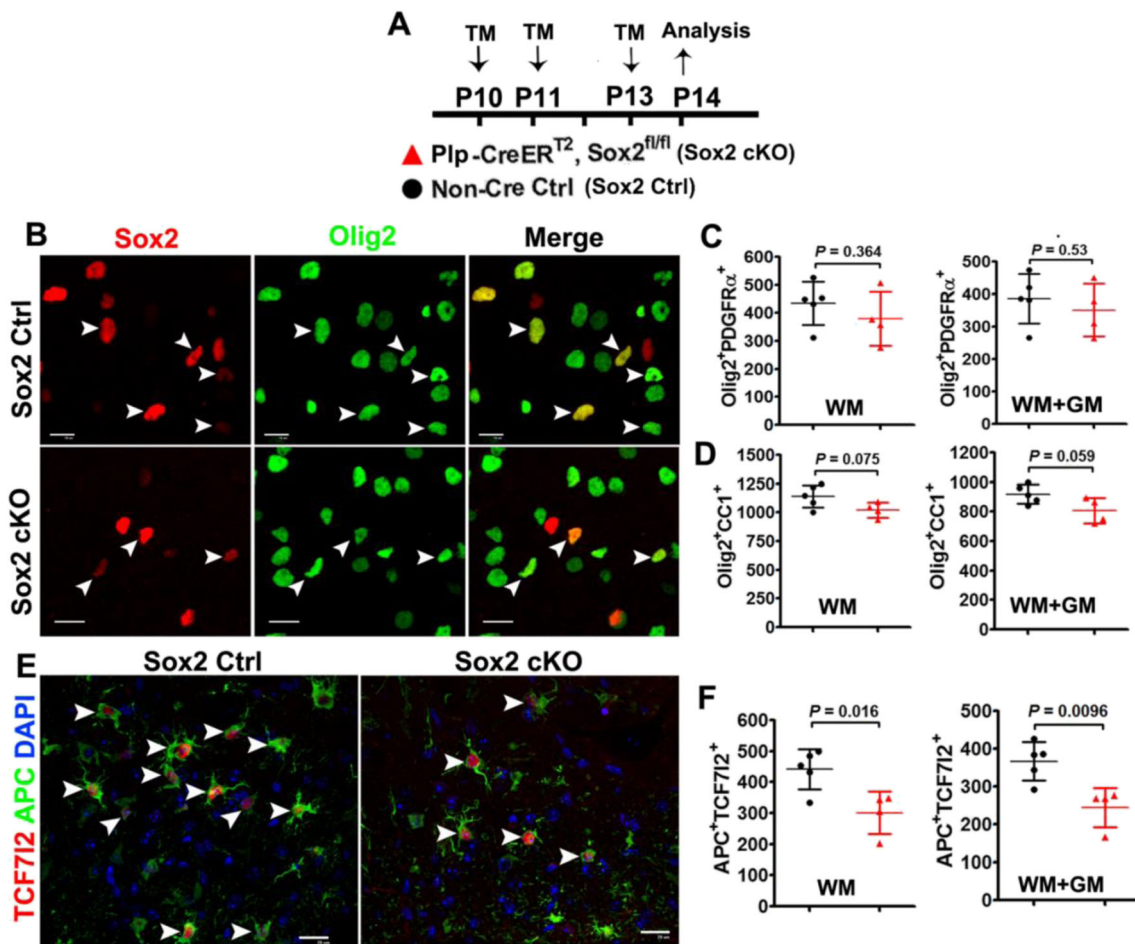


Fig. 10 Sox2 regulates the rate of oligodendrocyte production—evidences from *Plp-CreER^{T2}:Sox2^{fl/fl}* transgenic mice. **a** Transgenic mice and experimental designs for panels **b–f**. *Plp-CreER^{T2}:Sox2^{fl/fl}* (Sox2 cKO) and non-Cre Ctrl mice were injected intraperitoneally with tamoxifen at P10, P11, and P13 once a day and sacrificed 24 h after the last injection. **b** Representative confocal images showing Sox2 is expressed in Olig2⁺ oligodendroglial lineage cells in non-Cre Ctrl (upper panels, arrowheads) and absent from most Olig2⁺ cells in P14 spinal cord

of Sox2 cKO mice (lower panels, arrowheads). Scale bars = 10 μm . **c** Densities (per mm^2) of Olig2⁺PDGFR α ⁺ OPCs. Two-tailed Student's *t* test [$t_{(7)} = 0.972$ WM, $t_{(7)} = 0.661$ WM + GM]. **d** Densities (mm^2) of Olig2⁺CC1⁺ OPCs. Two-tailed Student's *t* test [$t_{(7)} = 2.088$ WM, $t_{(7)} = 2.258$ WM + GM]. **e** Representative confocal images showing reduction of APC⁺TCF712⁺ premyelinating OLs in P14 spinal cord. Scale bars = 10 μm . **f** Density (per mm^2) of APC⁺TCF712⁺ cells. Two-tailed Student's *t* test [$t_{(7)} = 3.163$ WM, $t_{(7)} = 3.528$ WM + GM]

dispensable for OL differentiation in the postnatal spinal cord, as concluded by previous study [10]. Alternatively, it is possible that Sox2 may regulate the timing of OL differentiation in the postnatal spinal cord. If this possibility happens, oligodendrocyte population should be reduced at some time points before P14. To this end, we analyzed oligodendrocyte differentiation and myelin gene expression at P8, the approximate peak of OL differentiation in the murine spinal cord, and found that OL differentiation and myelination are significantly decreased in the P8 spinal cord of *Cnp-Cre:Sox2^{fl/fl}* mutants. The time course analysis of *Cnp-Cre:Sox2^{fl/fl}* hybrids favors the latter possibility that Sox2 is an intrinsic positive timer regulating the timing of oligodendrocyte differentiation in the postnatal spinal cord. Another novel finding in the current study is that Sox2 regulates OPC proliferation in a developmental stage-dependent (embryonic vs spinal cord) manner.

Using *Sox10-Cre:Sox2^{fl/fl}* embryos, we confirmed that Sox2 does not regulate OPC proliferation in the embryonic spinal cord, a conclusion that is in line with the one by Hoffmann et al. [9]. Interestingly, our data show that Sox2 plays a crucial role in postnatal OPC proliferation in the spinal cord.

How Sox2 promotes oligodendrocyte differentiation and myelination is an open question. Sox2 is a transcription factor that either activates or silences its target genes depending on recruiting its partners of co-activators or co-repressors, respectively in different contexts [28–31]. Previous study suggests that Sox2 represses miR145, thus preventing miR145 from inhibiting several pro-differentiation factors [9]. Our preliminary study of co-immunoprecipitation in combination with mass spectrometry (CoIP-MS) showed that, in the Oli-neu oligodendrocyte cell line [32], Sox2 interacted with transcriptional repressors HDAC1/2 and YY1 and transcriptional

activators TCF712, and Olig1/2 (data not shown), all of which have been shown to promote oligodendrocyte differentiation and myelination [13, 15, 22, 33–35]. Recent ChIP-Seq data show that Sox2 may target the signaling pathways of Wnt, Akt, and Notch in the adult cerebral cortex [36], all of which have been shown to regulate OL differentiation and myelination [37]. Since Sox2-expressing cells in the adult cerebral cortex are astrocytes [36] and OPCs (Fig. 1d), it is not quite clear whether Sox2 targets these pathways in astrocytes or in OPCs. Further experimental data are needed to link Sox2 with those pathways, if any, in the context of oligodendroglial lineage cells, and importantly, how Sox2 modulates those pathways also warrants more investigations.

In summary, our data from genetic approaches unequivocally prove that the pluripotency factor Sox2 plays a crucial role in coordinating OPC proliferation and OL differentiation and is required for developmental myelination in the postnatal murine spinal cord. Our study provides justification that Sox2 may be a therapeutic target for overcoming OPC differentiation arrest in CNS dysmyelinating and demyelinating disorders.

Materials and Methods

Animals

Animals and procedures used in the study were covered and approved by the Institutional Animal Care and Use Committee (IACUC) of UC Davis. Animals were housed at 12 h light/dark cycle with access to food and drink, and both male and female mice were used in this study. All transgenic mice were crossed and maintained on a C57BL/6J background. The transgenic lines and their identification are as follows: *Sox2-CreER^{T2}* (RRID: IMSR_JAX:017593), *Pdgfr α -CreER^{T2}* (RRID: IMSR_JAX:018280), *Sox10-Cre* (RRID: IMSR_JAX:025807), *Cnp-Cre* (RRID: MGI_3051754), *Plp-CreER^{T2}* (RRID: IMSR_JAX:005617), *Sox2^{fl/fl}* (RRID: IMSR_JAX:013093), and *Rosa26-LoxP-STOP-LoxP-EYFP* (referred to as *Rosa-EYFP*) (RRID: IMSR_JAX:006148). All Cre lines including breeders and study mice were maintained as heterozygosity (i.e., Cre^{+/-}). In this study, Sox2 conditional knockout (cKO) mice were referred to as Cre^{+/-}:Sox2^{fl/fl} whereas non-Cre controls were referred to as Sox2^{fl/+} or Sox2^{fl/fl} that do not carry Cre transgene. For studies using timed pregnant mice (Fig. 2), we placed male and female mice into one cage around 5:00 pm in the late afternoon, and the female mice were designated as pregnancy if the sperm plugs were seen by 10:00 am of the next day, and the embryos were assigned as embryonic day 0.5 (E0.5). For postnatal studies, the day when pups were born was designated as postnatal day 0 (P0).

Tamoxifen, BrdU, and Edu Treatment

Tamoxifen (TM) (T5648; Sigma-Aldrich) was dissolved in mixture of ethanol and sunflower oil (1:9 by volume) at a concentration of 30 mg/ml [13, 14]. Tamoxifen was administered intraperitoneally to adult *Sox2-CreER^{T2}:Rosa-EYFP* mice (Fig. 1) at a dose of 1 mg (~35 μ l) daily for five consecutive days, subcutaneously to neonatal pups (*Pdgfr α -CreER^{T2}:Sox2^{fl/fl}* and non-Cre controls) on P1, P2, and P3 daily at a dose of 10 μ l (300 μ g) once a day (Fig. 6 and Fig. 7), and intraperitoneally to *Plp-CreER^{T2}:Sox2^{fl/fl}* and non-Cre controls daily on P10, P11, and P13 at a dose of 20 μ l (600 μ g) (Fig. 9). Animals were sacrificed at time points indicated in each figure. BrdU or EdU (10 mg/ml, dissolved in saline) was intraperitoneally injected to Sox2 cKO and control littermates at a dose of 100 μ g/g body weight 2 h prior to sacrifice.

Tissue Harvesting and Processing for Histology

After anesthetized by ketamine/xylazine mixture, mice were transcardially perfused with ice-cold PBS. Spinal cord was dissected out and immediately placed on dry ice (for protein or RNA extraction) or post-fixed in 4% paraformaldehyde (PFA) (for histological study). After post-fix in 4% PFA for 2 h at room temperature, the spinal cord was washed with PBS, three times, 15 min each time. Tissue samples were then cryoprotected in 30% sucrose (dissolved in PBS) for 20 h and cut into 16- μ m-thick sections on Leica Cryostats. Sections were stored under -80 °C until use for immunohistochemistry or mRNA in situ hybridization.

Immunohistochemistry and mRNA In Situ Hybridization

Immunohistochemistry (IHC) and mRNA in situ hybridization (ISH) were performed as previously described [13, 14]. The following antibodies were used in immunohistochemistry: Sox2 (sc-17320, RRID: AB_2286684, 1:500; Santa Cruz Biotechnology), Olig2 (AF2418, RRID: AB_2157554, 1:100; R&D Systems; AB9610, AB_10141047, 1:500; Millipore), CC1 (OP80, RRID: AB_213434, 1:200; Calbiochem), TCF712 (2569S, RRID: AB_2199816, 1:200; Cell Signaling Technology; sc-8632, RRID: AB_2199825, 1:100; Santa Cruz Biotechnology), PDGFR α (AF1062, AB_2236897, 1:200; R&D System), EYFP (06-896, RRID: AB_310288, 1:500; Millipore), NG2 (AB5320, RRID: AB_91789, 1:200; Millipore), Ki67 (9129, RRID: AB_10989986, 1:200; Cell Signaling Technology), Sox10 (sc-17342, RRID: AB_2195374, 1:100; Santa Cruz Biotechnology), BrdU (sc-70441, RRID: AB_1119696, 1:100; Santa Cruz Biotechnology), and APC (sc-896, RRID: AB_2057493, 1:100; Santa Cruz Biotechnology). DyLight 488- or DyLight 549-conjugated secondary antibodies were from

Jackson ImmunoResearch. Brdu and Edu (Click-iT Edu imaging kits, Invitrogen C10339) immunostaining were performed as in previous study [13, 14].

Protein Extraction and Western Blot

The frozen mouse spinal cord was homogenized in RIPA buffer (Cell Signaling Technology, #9806) supplemented with the protease/phosphatase inhibitor cocktail buffer (Cell Signaling Technology, #5872) and PMSF (Cell Signaling Technology, #8553) at a ratio of 100 mg of tissue to 1 ml of buffer. Lysates were sonicated, incubated on ice for 30 min, and centrifuged at 14,000g for 10 min. The supernatants were assessed for protein concentration using the BCA protein assay kit (Thermo Scientific, #23235). Western blot was performed according to the protocols in our previous studies [13, 14]. A total of 30 µg protein extracts was separated by anykD precast polyacrylamide gel (Bio Rad, #4569033) and transferred to nitrocellulose immobilization membranes (Bio Rad, #1704158) using Trans-Blot Turbo transfer system (Bio Rad, #1704150). Membranes were blocked for 1 h in 5% BSA (Cell Signaling Technology, #9998) at room temperature and incubated with the primary antibody overnight at 4 °C. Subsequently, membranes were washed three times 10 min each in TBST buffer (Tris 25 mM, KCl 3 mM, NaCl 140 mM, pH 7.4, and Tween 0.1%) and incubated with secondary antibodies for 1 h at room temperature. Membranes were washed three times in the same wash buffer, and detection was performed by exposing the membranes to PhosphorImager Screen (PHENIX, #F-BX57).

The following antibodies were used for Western blot: MBP (NB600-717, RRID: AB_2139899, 1:1000; Novus), Cnp (C5922, RRID: AB_823640, 1:1000; Sigma), and beta-actin (3700, RRID: AB_2242334, 1:1000; Cell Signaling Technology).

RNA Extraction, cDNA Preparation, and Real-Time Quantitative PCR (RT-qPCR)

Total spinal cord RNA was extracted by using the commercial isolation kit (Qiagen catalog#: 74804) with additional on-column DNase I digestion to eliminate genomic DNA contamination. RNA quality was assessed by Agilent Bioanalyzer 2100. Only RNAs with RNA Integrity Number (RIN) greater than 6.8 were used for subsequent complementary DNA (cDNA) preparation. cDNA was prepared by Qiagen Omniscript RT Kit (catalog#: 205111) with 2 µg RNA in 20 µl reaction buffer. The resulting 20 µl cDNA was further diluted with TE buffer (pH 8.0) to a total volume of 400 µl (380 µl TE buffer to 20 µl cDNA stock solution), and 1 µl of the diluted cDNA solution (equivalent to 5 ng RNA) was used as templates for RT-qPCR. We used Sybr green-based method (QIAGEN catalog#: 204143) for qPCR. In our study, the Ct

(cycle threshold) of the internal control gene Hsp90 was approximately 20–21. The mRNA levels of indicated genes were normalized to those of the Hsp90 and calculated by the equation $2^{-(Ct \text{ value for Hsp90} - Ct \text{ value for indicated genes})}$. The mRNA level in non-Cre control spinal cord was designated to 1. Most of the primer sets used in this study were from PrimerBank (<https://pga.mgh.harvard.edu/primerbank/>) and listed here as follows: *Hsp90* (F: AAACAAGGAGATTTTCCTCCGC, R: CCGTCAGGCTCTCATATCGAAT), *Sox2* (F: CGGCACAGATGCAACCGAT, R: CCGTTCATGTAGGTCTGCG), *Sox10* (F: ACACCTTGGGACACGGTTTTC, R: TAGGTCTTGTTCCCTCGGCCAT), *Mag* (F: CTGCCGCTGTTTTGGATAATGA, R: CATCGGGGAAGTCGAAACGG), *Enpp6* (F: CAGAGAGATTGTGAACAGAGGC, R: CCGATCATCTGTTGGACCT), *Bcas1* (F: AGAAGCGAAAGGCTCGGAAG, R: AGGGACAGATAACTCAGAGTGT), *Mbp* (F: GGCGGTGACAGACTCCAAG, R: GAAGCTCGTCGGACTCTGAG), *Cnp* (F: TTTACCCGCAAAAGCCACACA, R: CACCGTGTCTCATCTTGAAG), *Qc1* or *CC1* (F: CTGGACGAAGAAATTAGCAGAGT, R: ACTGCCATTTAACGTGCATTGT), *Ugt8a* (F: GAACATGGCTTTGTCCTGGT, R: CATGGCTTAGGAAGGCTCTG), *Plp-E3b* (targeting the exon 3b of *Plp1* gene, which is only expressed in myelinating OLs) (F: GTTCCAGAGGCCAACATCAAG, R: CTTGTCCGGATGTCTAGCC), *Mog* (F: AGCTGCTCCTCTCCCTTCTC, R: ACTAAAGCCCGGATGGGATAC), *Bmp4*: (F: TTCCTGGTAACCGAATGCTGA, R: CCTGAATCTCGGCGACTTTTTT), and *Tcf712* (F: GGAGGAGAAGAAGCTCGGAAAA, R: ATCGGAGGAGCTGTTTTGATT).

Confocal Image Acquisition and Quantification

Nikon laser-scanning confocal microscope was used to acquire confocal images. Laser settings remained consistent across different mouse genotypes of histological sections. Nikon EZ-C1 FreeViewer v3.90 was used for cell quantification and area calculation. To quantify cell density, four projected confocal images at 20× (oil lens) magnification (10 µm optical thickness from 11 consecutive stacked 1-µm confocal optical slices, ~330,000 µm² per 20× image) were obtained from same locations in the spinal cord of Sox2 cKO and non-Cre control mice. To increase the accuracy of OPC and OL quantification, we included the nuclear Sox10 (or Olig2) immunostaining with the OPC marker PDGFRα (or NG2) and the differentiated OL marker CC1. Only PDGFRα⁺ or CC1⁺ cells with nuclear Sox10 (or Olig2) signals were counted as individual OPCs or OLs. Similarly, to increase the accuracy of premyelinating OL quantification, we used double immunohistochemistry of the cell surface antigen APC and the nuclear antigen TCF712. Only APC⁺ cells with nuclear TCF712 signals were counted as individual

premyelinating OLs. The NIH ImageJ software was used to quantify the relative intensity of MBP and SMI312 immunoreactivity.

Accelerating Rotarod Test

Motor performance and coordination were measured by accelerating rotarod test machine (Columbus instruments, Rotamex-5 Rota rod). The following parameter settings were used: starting speed 4 rotations per minute (rpm), speed increased by 1.2 rpm every 10 s, maximal speed 40 rpm. The retention time was recorded for each mouse which is defined as the time duration that a mouse is retained on the rotating rods prior to falling off.

Semi-Thin Section Preparation and Toluidine Blue Staining of Myelin

Mice were anesthetized by ketamine/xylazine mixture, then perfused with 60 ml 4% paraformaldehyde (dilute with phosphate buffer, EMS, 11601-40, pH 7.4) and 60 ml 3% glutaraldehyde (Electron Microscopy Science, 16130, dilute in PBS, pH 7.4) at a speed of 5 ml per minute. Spinal cord was carefully dissected out and fixed with 3% glutaraldehyde overnight followed by wash with sodium cacodylate (Electron Microscopy Science, EMS, 11653) twice, 10 min each time, and then post-fixed with 2% (*w/v*) osmium tetroxide (Electron Microscopy Science, 19152) for 1.5 h and wash with sodium cacodylate twice, 10 min each time. The resulting spinal cord was dehydrated with gradient ethanol of 50, 70, 90, and 100% followed by wash with propylene oxide for three times, 30 min each time, and incubation with 1:1 mixture of propylene oxide:Eponate resin overnight, and with 3:1 mixture of propylene oxide:Eponate resin for 10 h, and incubation with 100% Eponate resin overnight. Transverse sections were embedded in EMBED812-Resin for 2 days at 65°. Semi-thin (500 nm) were cut by using a Leica EM UC7 microtome. Semi-thin sections were dry and incubated with 2% toluidine blue (Cat#19451, Ted Pella Inc.) at 100 °C for 2 min, followed by imaging on Olympus BX61 microscope.

Statistical Analyses

Quantification was performed by blinded observers. At least three sections from each mouse were used, and 3–7 mice were quantified. Data were presented as mean \pm s.d. except stated otherwise. We used graphs of scatter plots to present the quantification data throughout our manuscript, and each circle, square, or triangle represents one mouse. *Shapiro-Wilk* approach was used for testing data normality. The statistical methods were described in the figure legends. For two-tailed Student's *t* test, *P* value was presented in each graph, and *t* value and degree of freedom (*df*) were presented as $t_{(df)}$ in

figure legends. Welch's correction was used in Student's *t* test if the variance of two groups of datasets was not equal. For comparisons among three or more groups, one-way *ANOVA* followed by Tukey's post-hoc test was used. We used GraphPad Prism version 5.0 to perform all statistical analyses and data plotting. *P* value less than 0.05 was considered as significant. ns stands for not significant with *P* value greater than 0.05.

Acknowledgements Grant support was from Shriners Hospitals for Children (F.G., S.Z.), 2016YFC0503200 (X. Z.), and NIH (R01NS094559, R21NS093559 to F.G.).

References

- Franklin RJ, Gallo V (2014) The translational biology of remyelination: past, present, and future. *Glia* 62:1905–1915
- Graham V, Khudyakov J, Ellis P, Pevny L (2003) SOX2 functions to maintain neural progenitor identity. *Neuron* 39(5):749–765
- Lee KE, Seo J, Shin J, Ji EH, Roh J, Kim JY, Sun W, Muhr J et al (2014) Positive feedback loop between Sox2 and Sox6 inhibits neuronal differentiation in the developing central nervous system. *Proc Natl Acad Sci U S A* 111(7):2794–2799
- Kondo T, Raff M (2004) Chromatin remodeling and histone modification in the conversion of oligodendrocyte precursors to neural stem cells. *Genes Dev* 18(23):2963–2972
- Lyssiotis CA, Walker J, Wu C, Kondo T, Schultz PG, Wu X (2007) Inhibition of histone deacetylase activity induces developmental plasticity in oligodendrocyte precursor cells. *Proc Natl Acad Sci U S A* 104(38):14982–14987
- Niu W, Zang T, Zou Y, Fang S, Smith DK, Bachoo R, Zhang CL (2013) In vivo reprogramming of astrocytes to neuroblasts in the adult brain. *Nat Cell Biol* 15(10):1164–1175
- Su Z et al (2014) In vivo conversion of astrocytes to neurons in the injured adult spinal cord. *Nat Commun* 5:3338
- Heinrich C, Bergami M, Gascón S, Lepier A, Viganò F, Dimou L, Sutor B, Berninger B et al (2014) Sox2-mediated conversion of NG2 glia into induced neurons in the injured adult cerebral cortex. *Stem Cell Reports* 3(6):1000–1014
- Hoffmann SA, Hos D, Kuspert M, Lang RA, Lovell-Badge R, Wegner M, Reiprich S (2014) Stem cell factor Sox2 and its close relative Sox3 have differentiation functions in oligodendrocytes. *Development* 141(1):39–50
- Zhao C, Ma D, Zawadzka M, Fancy SPJ, Elis-Williams L, Bouvier G, Stockley JH, de Castro GM et al (2015) Sox2 sustains recruitment of oligodendrocyte progenitor cells following CNS demyelination and primes them for differentiation during remyelination. *J Neurosci* 35(33):11482–11499
- Zhang S, Zhu X, Gui X, Croteau C, Song L, Xu J, Wang A, Bannerman P et al (2018) Sox2 is essential for oligodendroglial proliferation and differentiation during postnatal brain myelination and CNS remyelination. *J Neurosci* 38:1802–1820
- Stolt CC, Rehberg S, Ader M, Lommes P, Riethmacher D, Schachner M, Bartsch U, Wegner M (2002) Terminal differentiation of myelin-forming oligodendrocytes depends on the transcription factor Sox10. *Genes Dev* 16(2):165–170
- Hammond E, Lang J, Maeda Y, Pleasure D, Angus-Hill M, Xu J, Horiuchi M, Deng W et al (2015) The Wnt effector transcription factor 7-like 2 positively regulates oligodendrocyte differentiation in a manner independent of Wnt/beta-catenin signaling. *J Neurosci* 35(12):5007–5022

14. Lang J, Maeda Y, Bannerman P, Xu J, Horiuchi M, Pleasure D, Guo F (2013) Adenomatous polyposis coli regulates oligodendroglial development. *J Neurosci: Off J Soc Neurosci* 33(7):3113–3130
15. Zhao C, Deng Y, Liu L, Yu K, Zhang L, Wang H, He X, Wang J et al (2016) Dual regulatory switch through interactions of Tcf7l2/Tcf4 with stage-specific partners propels oligodendroglial maturation. *Nat Commun* 7:10883
16. Dugas JC, Cuellar TL, Scholze A, Ason B, Ibrahim A, Emery B, Zamanian JL, Foo LC et al (2010) Dicer1 and miR-219 are required for normal oligodendrocyte differentiation and myelination. *Neuron* 65(5):597–611
17. Moyon S, Huynh JL, Dutta D, Zhang F, Ma D, Yoo S, Lawrence R, Wegner M et al (2016) Functional characterization of DNA methylation in the oligodendrocyte lineage. *Cell Rep* 15:748–760
18. Moyon S, Casaccia P (2017) DNA methylation in oligodendroglial cells during developmental myelination and in disease. *Neurogenesis (Austin)* 4(1):e1270381
19. Ishii A, Fyffe-Maricich SL, Furusho M, Miller RH, Bansal R (2012) ERK1/ERK2 MAPK signaling is required to increase myelin thickness independent of oligodendrocyte differentiation and initiation of myelination. *J Neurosci* 32(26):8855–8864
20. Ishii A, Furusho M, Bansal R (2013) Sustained activation of ERK1/2 MAPK in oligodendrocytes and Schwann cells enhances myelin growth and stimulates oligodendrocyte progenitor expansion. *J Neurosci* 33(1):175–186
21. Marques S, Zeisel A, Codeluppi S, van Bruggen D, Mendanha Falcao A, Xiao L, Li H, Haring M et al (2016) Oligodendrocyte heterogeneity in the mouse juvenile and adult central nervous system. *Science* 352(6291):1326–1329
22. Dai J, Bercury KK, Ahrendsen JT, Macklin WB (2015) Olig1 function is required for oligodendrocyte differentiation in the mouse brain. *J Neurosci* 35(10):4386–4402
23. Shen S, Sandoval J, Swiss VA, Li J, Dupree J, Franklin RJM, Casaccia-Bonnel P (2008) Age-dependent epigenetic control of differentiation inhibitors is critical for remyelination efficiency. *Nat Neurosci* 11(9):1024–1034
24. Fernandez-Castaneda A, Gaultier A (2016) Adult oligodendrocyte progenitor cells—multifaceted regulators of the CNS in health and disease. *Brain Behav Immun* 57:1–7
25. Young KM, Psachoulia K, Tripathi RB, Dunn SJ, Cossell L, Attwell D, Tohyama K, Richardson WD (2013) Oligodendrocyte dynamics in the healthy adult CNS: evidence for myelin remodeling. *Neuron* 77(5):873–885
26. Xiao L, Ohayon D, McKenzie IA, Sinclair-Wilson A, Wright JL, Fudge AD, Emery B, Li H et al (2016) Rapid production of new oligodendrocytes is required in the earliest stages of motor-skill learning. *Nat Neurosci* 19(9):1210–1217
27. Tripathi RB, Jackiewicz M, McKenzie IA, Kougoumtzidou E, Grist M, Richardson WD (2017) Remarkable stability of myelinating oligodendrocytes in mice. *Cell Rep* 21(2):316–323
28. Reiprich S, Wegner M (2014) From CNS stem cells to neurons and glia: Sox for everyone. *Cell Tissue Res*
29. Reiprich S, Wegner M (2014) Sox2: a multitasking networker. *Neurogenesis (Austin)* 1(1):e962391
30. Liu YR, Laghari ZA, Novoa CA, Hughes J, Webster JRM, Goodwin PE, Wheatley SP, Scotting PJ (2014) Sox2 acts as a transcriptional repressor in neural stem cells. *BMC Neurosci* 15:95
31. Engelen E, Akinci U, Bryne JC, Hou J, Gontan C, Moen M, Szumska D, Kockx C et al (2011) Sox2 cooperates with Chd7 to regulate genes that are mutated in human syndromes. *Nat Genet* 43(6):607–611
32. Jung M, Krämer E, Grzenkowski M, Tang K, Blakemore W, Aguzzi A, Khazaie K, Chlichlia K et al (1995) Lines of murine oligodendroglial precursor cells immortalized by an activated neu tyrosine kinase show distinct degrees of interaction with axons in vitro and in vivo. *Eur J Neurosci* 7(6):1245–1265
33. He Y, Dupree J, Wang J, Sandoval J, Li J, Liu H, Shi Y, Nave KA et al (2007) The transcription factor Yin Yang 1 is essential for oligodendrocyte progenitor differentiation. *Neuron* 55(2):217–230
34. Ye F, Chen Y, Hoang TN, Montgomery RL, Zhao XH, Bu H, Hu T, Taketo MM et al (2009) HDAC1 and HDAC2 regulate oligodendrocyte differentiation by disrupting the beta-catenin-TCF interaction. *Nat Neurosci* 12(7):829–838
35. Lu QR, Sun T, Zhu Z, Ma N, Garcia M, Stiles CD, Rowitch DH (2002) Common developmental requirement for Olig function indicates a motor neuron/oligodendrocyte connection. *Cell* 109(1):75–86
36. Chen C et al (2017) Astrocyte-specific deletion of Sox2 promotes functional recovery after traumatic brain injury. *Cereb Cortex*:1–16
37. Wheeler NA, Fuss B (2016) Extracellular cues influencing oligodendrocyte differentiation and (re)myelination. *Exp Neurol* 283(Pt B):512–530